

Figure S1: Differential cargo trafficking effects following glucose starvation. **a)** Wild-type cells expressing Mup1-GFP were grown to mid-log phase in SC media lacking methionine, processed for time-lapse microscopy and then imaged every 2 minutes following addition of 20 $\mu\text{g/ml}$ methionine. **b)** Vacuolar GFP bleaching in wild-type cells expressing Mup1-GFP grown to mid-log phase in SC media lacking methionine and processed for time-lapse microscopy. Area 1 was imaged before addition of methionine, before moving to a distinct region of the same plate (Area 2) for continuous imaging from 0 – 53 minutes of methionine addition. Following this period, Area 1 was re-visited and imaged to show the difference in photobleaching of vacuolar sorted Mup1-GFP. **c)** Levels of vacuolar processed GFP from cargo (Mup1-GFP, left and Can1-GFP, right) expressing cells were assessed in glucose and raffinose treated cells by immunoblotting lysates with GFP antibodies. Loading was assessed with anti-GAPDH antibodies. **d)** Wild-type cells expressing Yor1-GFP from the *CUP1* promoter by addition of 50 μM copper chloride were grown to mid-log phase in glucose containing media, processed for time-lapse microscope and imaged for indicated time course after exchange with raffinose media. **e)** Strains expressing GFP tagged Hxt6 and Hxt7 expressed from the *NOP1* promoter were grown in glucose or raffinose media for indicated periods prior to fluorescence microscopy. **f)** Wild-type cells grown either in glucose media or exchanged with raffinose for 15 minutes were incubated with YPD containing 40 μM FM4-64 dye for 4 minutes at room temperature before ice cold washes were performed with minimal media to remove excess dye. Mean fluorescence of $\sim 10,000$ cells was then measured by flow cytometry, plotted with coefficient of variation (cv) indicated. Scale bar, 5 μm .

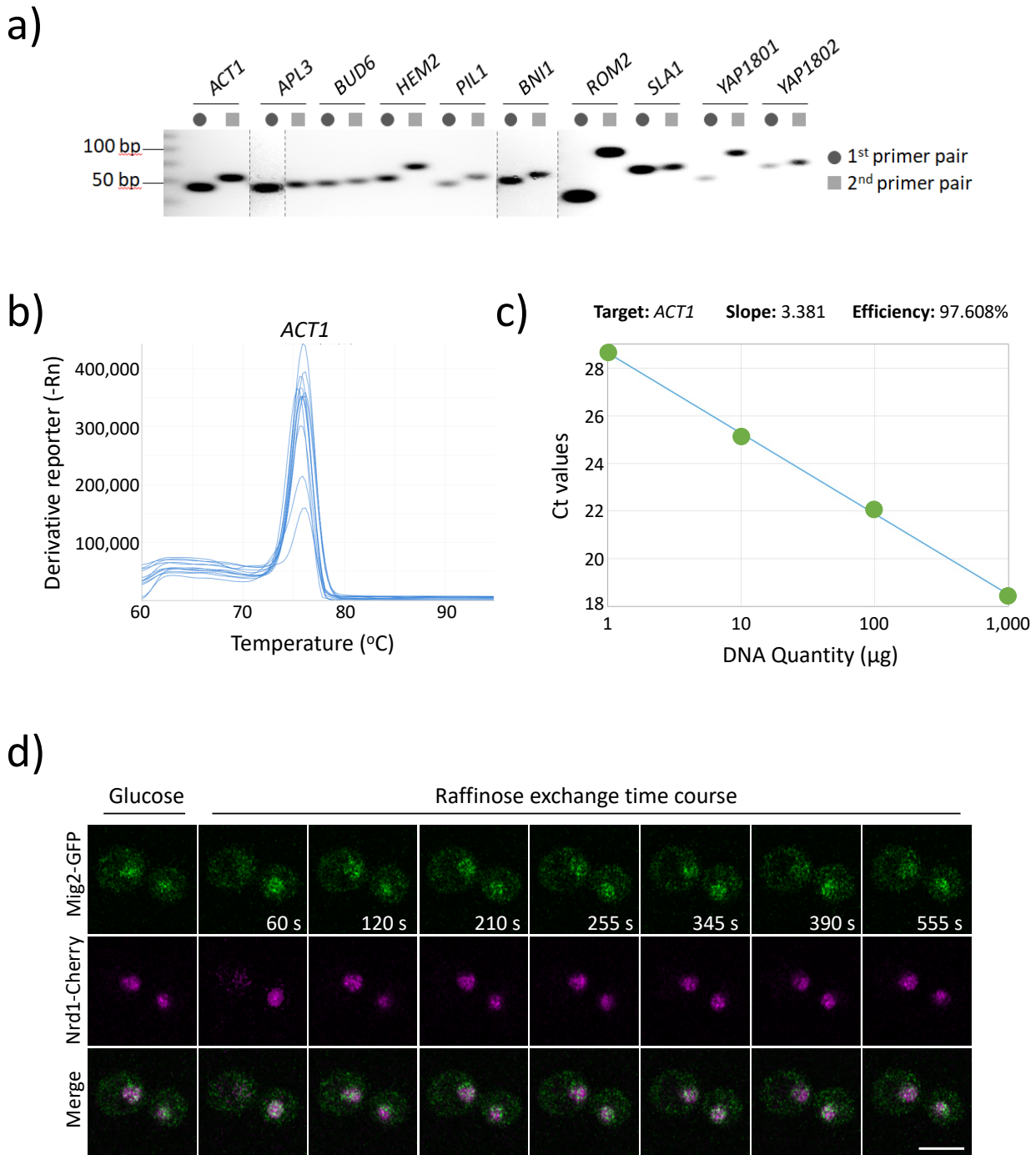


Figure S2: qPCR optimisation and time-lapse microscopy of Mig2-GFP: **a)** Indicated oligo pairs were used to generate PCR products from a gDNA template and analysed by agarose gel of primer pair validation of the qPCR using wild-type cells mRNA. **b)** Melt curve analyses for all qPCR primer pairs were carried out to ensure no primer dimer species were detected, read out shows example for ACT1. **c)** Primer pair efficiency was also performed for all primer pairs used in this study (shown for ACT1), with Δ Ct values across a 10-fold serial dilution plotted (slope = -3.33 equivalent to 100% efficiency). Data for all primer pair analysis is recorded in Supplemental Tables S2 & S3. **d)** Wild-type cells expressing Mig2-GFP and Nrd1-mCherry were grown to mid log phase in minimal media prior to processed for time-lapse microscopy. Images were captured every 5 seconds following raffinose exchange, with representative time-slices shown. Scale bar, 5 μ M.

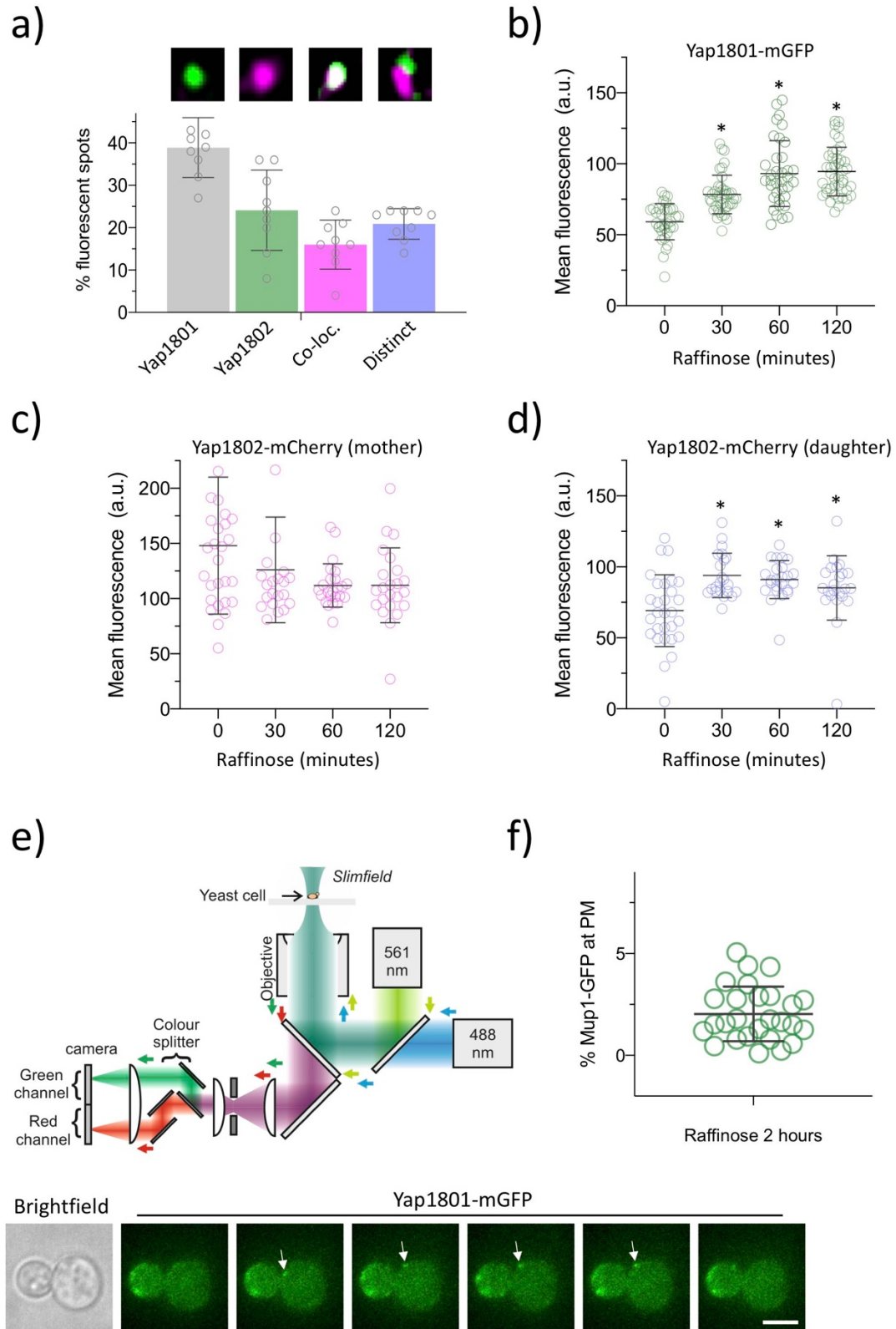


Figure S3: Localisation of Yap1801 and Yap1802: **a)** Histogram showing the co-localisation analysis of Airyscan confocal images of Yap1801-mGFP and Yap1802-mCherry expressing wild-type cells grown to mid-log phase in SC selective media. Error bars showing standard deviation (n = 235 foci analysed). Examples of each localisation category is shown (upper). **b-d)** Histograms showing mean fluorescence from confocal images cells grown in indicated media conditions whilst expressing **b)** Yap1801-mGFP (total cell), **c)** Yap1802-mCherry (just mother cell), **d)** Yap1802-mCherry (just daughter cell). Intensity was averaged from n=>36 cells per condition over 3 biological replicates, with error bars showing standard deviation. **e)** Slimfield microscopy, schematic diagram showing set-up for dual-colour imaging of yeast cells. Lower panels show Yap1801-mGFP fluorescent spot (white arrow) tracking from images acquired every 5ms. **f)** Percentage plasma membrane localised Mup1-GFP was calculated from cells grown in raffinose for two hours. * indicates Student t-test p-values <0.05. Scale bar, 5 μM.

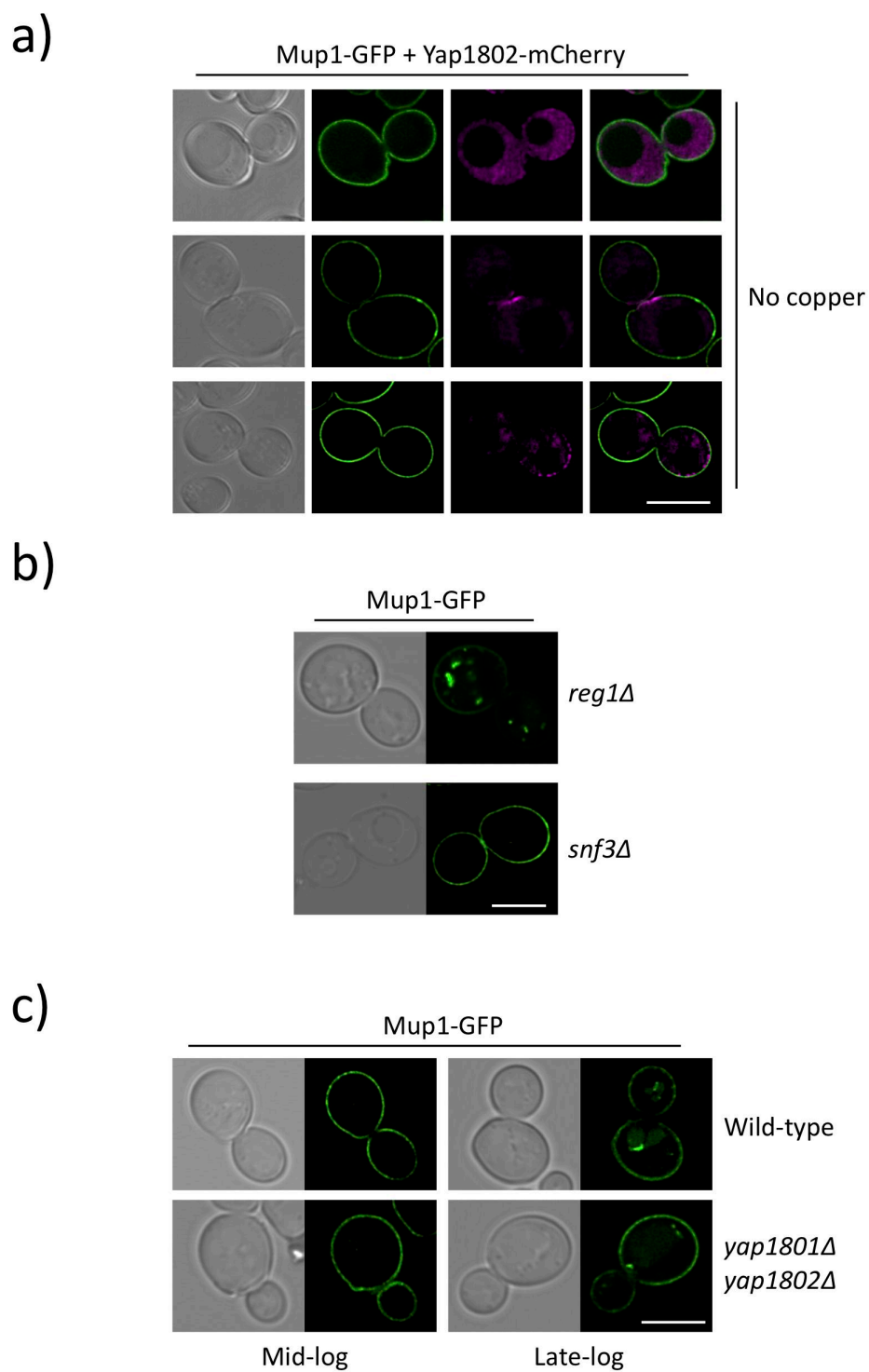


Figure S4: Functional relationship between Mup1-GFP trafficking and yeast AP180s: a) Representative examples of different Yap1802-mCherry localisations are shown from expression under the *CUP1* promoter with no additional copper added to the media, in cells co-expressing Mup1-GFP. b) Indicated mutant null strains expression Mup1-GFP were imaged by confocal microscopy. c) Mup1-GFP localisation was imaged in wild-type and *yap1801Δ yap1802Δ* cells grown to mid-log ($OD_{600} = 1.0$) and late-log ($OD_{600} = 2.0$) phase.

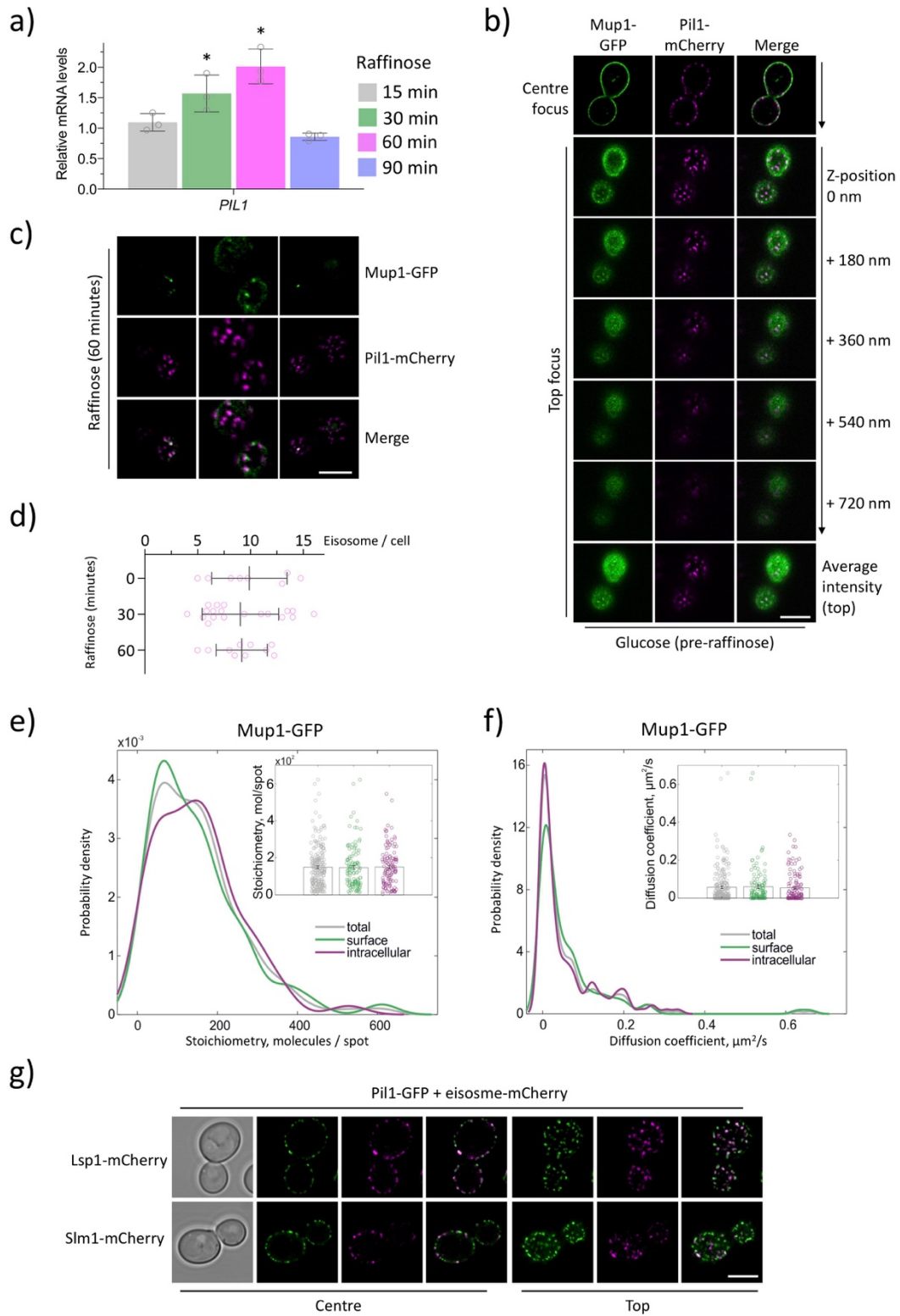


Figure S5: Analyses of eisosomes in response to changes in glucose levels: a) Quantitative RT-PCR of *PIL1* performed from RNA extracted from wild-type cells grown in glucose media and relative levels compared to cells grown in raffinose media for indicated time course. Error bars show the standard deviation from 3 biological replicates (each averaged from 3 technical replicates). b) Wild-type cells expressing Pil1-mCherry and Mup1-GFP were grown to mid-log phase in SC media and prepared for confocal imaging. Cells were focussed to the top of the cell and imaged at 0.18 μm intervals in the z-axis. An average intensity projection from the indicated 5 slices is shown (lower panel). c) Top focus 3D confocal imaging of cells expressing Mup1-GFP and Pil1-mCherry after 60 minutes raffinose starvation. d) Number of Pil1-mCherry marked eisosomes per cell in glucose, 30-minutes or 60-minutes raffinose and depicted with standard deviation error bars. e) Kernel density plots of Mup1-GFP stoichiometry distribution of fluorescent foci in the whole cell (grey), on the surface (green) or inside the cell (purple). Inserts: jitter plots of stoichiometries of fluorescent foci detected in the whole cell, on the surface or inside the cell. Error bars represent standard error. f) Kernel density plots of Mup1-GFP diffusion coefficients, using same labelling as (e) for total, surface and intracellular signal. g) Cells co-expressing Pil1-GFP with either Lsp1-mCherry (upper) or Slm1-mCherry (lower) were imaged at centre and top focus by confocal microscopy. * indicates Student t-test p-values < 0.05 . Scale bar, 5 μm

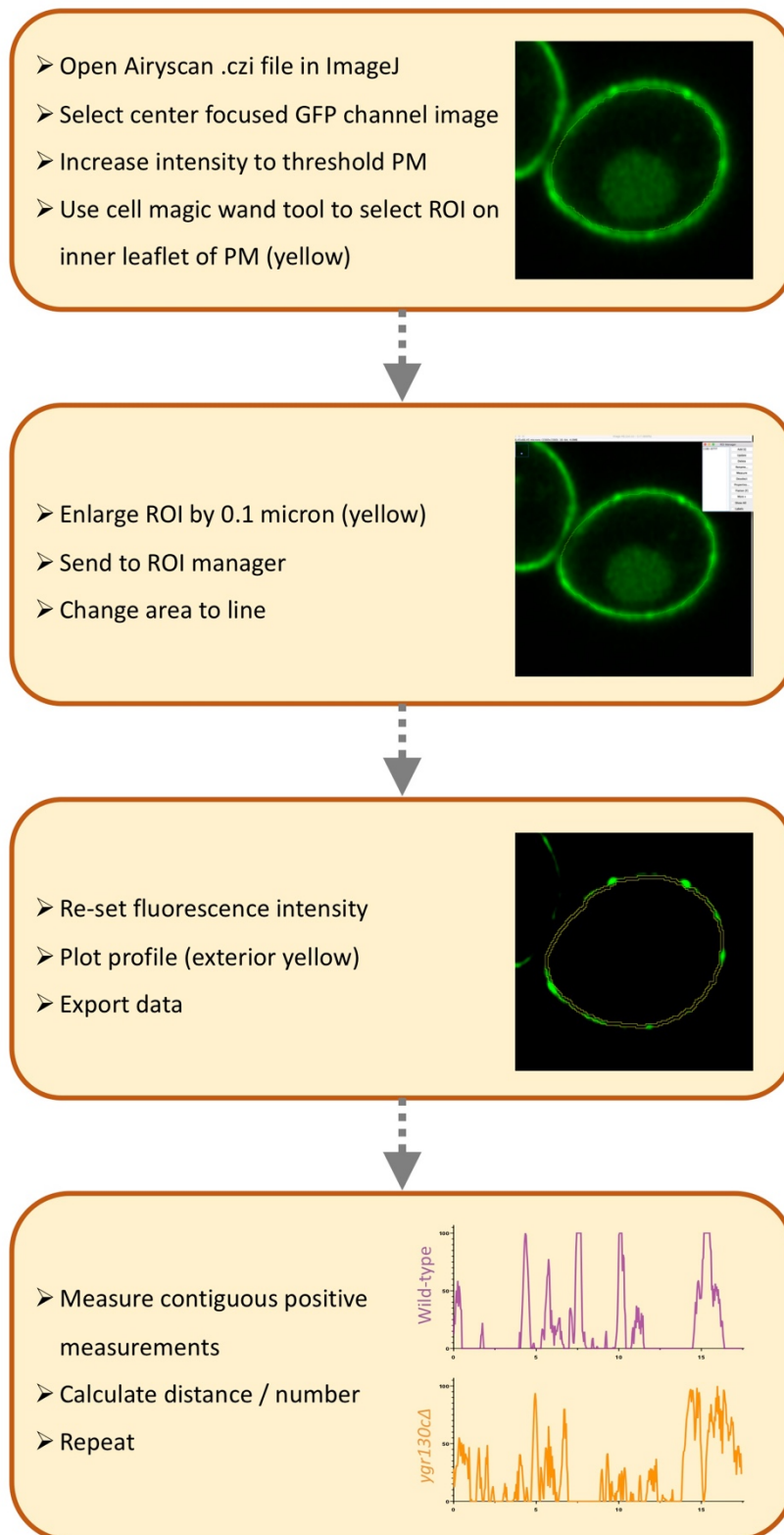


Figure S6: Analyses of eisosomes in response to changes in glucose levels: Workflow for systematic image processing used to measure the length of contiguous GFP signal at the plasma membrane in wild-type and *ygr130Δ* yeast cells expressing Mup1-GFP.

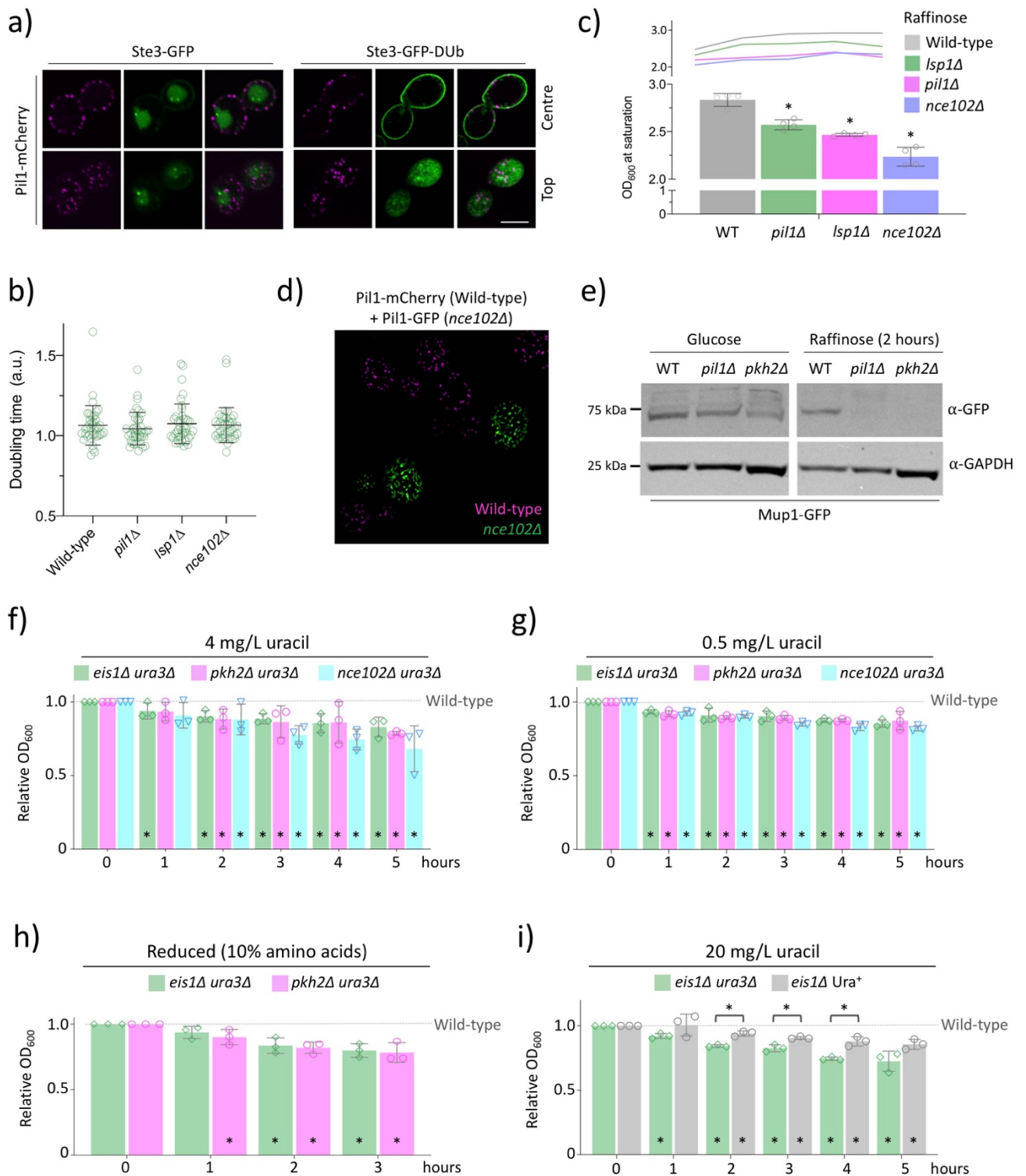


Figure S7: The role of eisosomes in cargo specific retention following starvation. **a)** Wild-type cells co-expressing Pil1-mCherry and either Ste3-GFP (left) or Ste3-GFP-DUB (right) were imaged by 3D confocal Airyscan microscopy. **b)** Indicated strains were grown to mid-log phase overnight and allowed to reach saturation, with OD₆₀₀ measurements captured every hour, depicted as a line graph (upper), or the maximum OD₆₀₀ shown as a histogram (lower). **c)** Triplicate cultures were grown to mid-log phase overnight, diluted to low optical density and then grown in 5ml cultures. Samples were taken for OD₆₀₀ measurements every hour over 8 – 10 hours and used to calculate average doubling times, with distribution displayed in scatter plot. **d)** Wild-type cells expressing Pil1-mCherry were co-cultured with *nce102Δ* cells expressing Pil1-GFP before Airyscan microscopy and merging colour channels. **e)** Indicated strains expressing Mup1-GFP were grown in either glucose (left) or 2 hours raffinose (right) media before denatured lysates generated and analysed by SDS-PAGE and immunoblot with antibodies against GFP and GAPDH. **f-i)** Indicated strains were grown to mid-log phase before incubation in raffinose media for two hours. Cells were then resuspended in SC media containing glucose and 4 mg/L Uracil (**f**), 0.5 mg/L Uracil (**g**), SC-media supplemented with only 10% amino acids or (**h**) 20 mg/L Uracil before OD₆₀₀ measurements recorded at 1-hour intervals during recovery period, depicted as histogram. Error bars show standard deviation from 3 biological replicates. * indicates Student t-test p-values <0.05. Scale bar, 5 μm.

Table S1: Functional clustering of Mig1 candidates

[Click here to Download Table S1](#)

Table S2: Ygr130c interactome

[Click here to Download Table S2](#)

Table S3: Mup1 interactome

[Click here to Download Table S3](#)

Table S4: Yeast Strains used in this study

[Click here to Download Table S4](#)

Table S5: Plasmids used in this study

[Click here to Download Table S5](#)

Table S6: qPCR primers

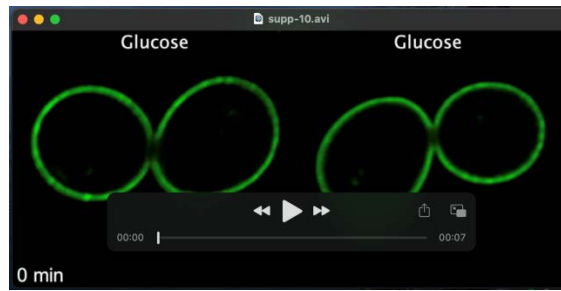
[Click here to Download Table S6](#)

Table S7: Primer efficiency and usage

[Click here to Download Table S7](#)

Table S8: Statistical analyse

[Click here to Download Table S8](#)



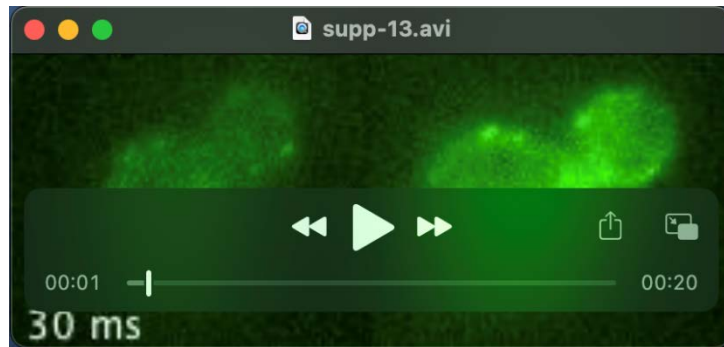
Movie 1: **Mup1-GFP endocytosis is triggered in raffinose, but not glucose, media**



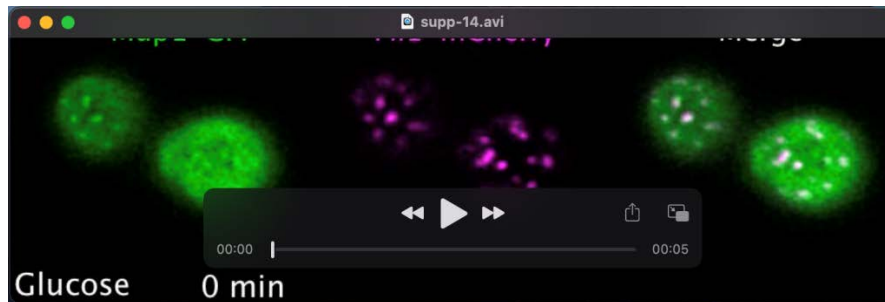
Movie 2: **Endocytic trafficking of Fur4-mNG / Ste3-GFP following raffinose exchange**



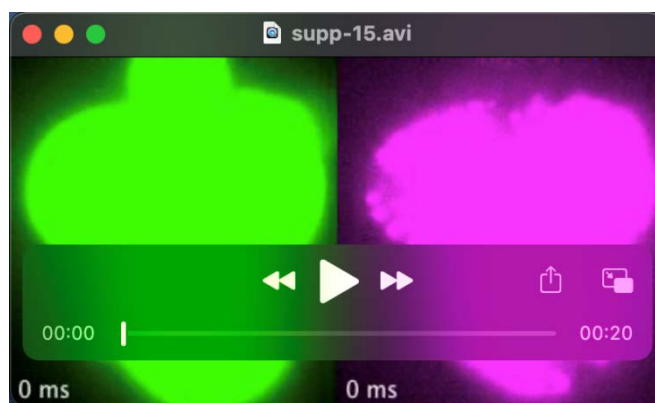
Movie 3: **Raffinose exchange triggers Mig1-mGFP translocation from Nrd1-mCherry labelled nuclei**



Movie 4: Slimfield acquisition of cells expressing mGFP tagged versions of Yap1801 and Yap1802



Movie 5: Mup1-GFP accumulates in Pil1-mCherry eisosomes following raffinose exchange



Movie 6: Slimfield acquisition of cells co-expressing Mup1-GFP and Pil1-mCherry

SUPPLEMENTAL REFERENCES

- Adell, M. A. Y., Migliano, S. M., Upadhyayula, S., Bykov, Y. S., Sprenger, S., Pakdel, M., Vogel, G. F., Jih, G., Skillern, W., Behrouzi, R., et al.** (2017). Recruitment dynamics of ESCRT-III and Vps4 to endosomes and implications for reverse membrane budding. *Elife* **6**, e31652.
- Brachmann, C. B., Davies, A., Cost, G. J., Caputo, E., Li, J., Hieter, P. and Boeke, J. D.** (1998). Designer deletion strains derived from *Saccharomyces cerevisiae* S288C: a useful set of strains and plasmids for PCR-mediated gene disruption and other applications. *Yeast* **14**, 115–132.
- MacDonald, C., Payne, J. A., Aboian, M., Smith, W., Katzmann, D. J. and Piper, R. C.** (2015). A Family of Tetraspans Organizes Cargo for Sorting into Multivesicular Bodies. *Dev Cell* **33**, 328–342.
- Robinson, J. S., Klionsky, D. J., Banta, L. M. and Emr, S. D.** (1988). Protein sorting in *Saccharomyces cerevisiae*: isolation of mutants defective in the delivery and processing of multiple vacuolar hydrolases. *Molecular and Cellular Biology* **8**, 4936–4948.
- Sikorski, R. S. and Hieter, P.** (1989). A system of shuttle vectors and yeast host strains designed for efficient manipulation of DNA in *Saccharomyces cerevisiae*. *Genetics* **122**, 19–27.
- Stringer, D. K. and Piper, R. C.** (2011). A single ubiquitin is sufficient for cargo protein entry into MVBs in the absence of ESCRT ubiquitination. *J Cell Biology* **192**, 229–242.
- Urbanowski, J. L. and Piper, R. C.** (2001). Ubiquitin Sorts Proteins into the Intraluminal Degradative Compartment of the Late-Endosome/Vacuole. *Traffic* **2**, 622–630.
- Weill, U., Yofe, I., Sass, E., Stynen, B., Davidi, D., Natarajan, J., Ben-Menachem, R., Avihou, Z., Goldman, O., Harpaz, N., et al.** (2018). Genome-wide SWAp-Tag yeast libraries for proteome exploration. *Nat Methods* **15**, 617–622.
- Winzeler, E. A., Shoemaker, D. D., Astromoff, A., Liang, H., Anderson, K., Andre, B., Bangham, R., Benito, R., Boeke, J. D., Bussey, H., et al.** (1999). Functional characterization of the *S. cerevisiae* genome by gene deletion and parallel analysis. *Science* **285**, 901–906.
- Wollman, A. J., Shashkova, S., Hedlund, E. G., Friemann, R., Hohmann, S. and Leake, M. C.** (2017). Transcription factor clusters regulate genes in eukaryotic cells. *Elife* **6**, e27451.
- Xu, P., Hankins, H. M., MacDonald, C., Erlinger, S. J., Frazier, M. N., Diab, N. S., Piper, R. C., Jackson, L. P., MacGurn, J. A. and Graham, T. R.** (2017). COPI mediates recycling of an exocytic SNARE by recognition of a ubiquitin sorting signal. *Elife* **6**, e28342.